catalysts

MDPI

Article

Hypercrosslinked Ionic Polymers with High Ionic Content for Efficient Conversion of Carbon Dioxide into Cyclic Carbonates

Xu Liao [1,†], Baoyou Pei [2,†], Ruixun Ma [2], Lingzheng Kong [2], Xilin Gao [1], Jiao He [1], Xiaoyan Luo [1,*] and Jinqing Lin [1,*]

[1] College of Materials Science and Engineering, Huaqiao University, Xiamen 361021, China; liaoxu@stu.hqu.edu.cn (X.L.); gaoxilin@stu.hqu.edu.cn (X.G.); hejiao@stu.hqu.edu.cn (J.H.)
[2] College of Chemical Engineering, Huaqiao University, Xiamen 361021, China; pbylt1314@stu.hqu.edu.cn (B.P.); maruixun@foxmail.com (R.M.); konglingzheng@stu.hqu.edu.cn (L.K.)
* Correspondence: chemistrylxy@163.com (X.L.); linlab@hqu.edu.cn (J.L.)
† These authors contributed equally to this work.

Abstract: The effective conversion of carbon dioxide (CO_2) into cyclic carbonates requires porous materials with high ionic content and large specific surface area. Herein, we developed a new systematic post-synthetic modification strategy for synthesizing imidazolium-based hypercrosslinked ionic polymers (HIPs) with high ionic content (up to 2.1 mmol g^{-1}) and large specific surface area (385 m^2 g^{-1}) from porous hypercrosslinked polymers (HCPs) through addition reaction and quaternization. The obtained HIPs were efficient in CO_2 capture and conversion. Under the synergistic effect of high ionic content, large specific surface area, and plentiful micro/mesoporosity, the metal-free catalyst [HCP-CH_2-Im][Cl]-1 exhibited quantitative selectivities, high catalytic yields, and good substrate compatibility for the conversion of CO_2 into cyclic carbonates at atmospheric pressure (0.1 MPa) in a shorter reaction time in the absence of cocatalysts, solvents, and additives. High catalytic yields (styrene oxide, 120 °C, 8 h, 94% yield; 100 °C, 20 h, 93% yield) can be achieved by appropriately extending the reaction times at low temperature, and the reaction times are shorter than other porous materials under the same conditions. This work provides a new strategy for synthesizing an efficient metal-free heterogeneous catalyst with high ionic content and a large specific surface area from HCPs for the conversion of CO_2 into cyclic carbonates. It also demonstrates that the ionic content and specific surface area must be coordinated to obtain high catalytic activity for CO_2 cycloaddition reaction.

Keywords: hypercrosslinked ionic polymers; high ionic content; CO_2 cycloaddition; cyclic carbonates

check for updates

Citation: Liao, X.; Pei, B.; Ma, R.; Kong, L.; Gao, X.; He, J.; Luo, X.; Lin, J. Hypercrosslinked Ionic Polymers with High Ionic Content for Efficient Conversion of Carbon Dioxide into Cyclic Carbonates. *Catalysts* **2022**, *12*, 62. https://doi.org/10.3390/catal12010062

Academic Editors: Vincenzo Vaiano and Olga Sacco

Received: 28 November 2021
Accepted: 31 December 2021
Published: 6 January 2022

1. Introduction

The exploitation of effective strategies for CO_2 capture, sequestration, and utilization is crucial for the sustainable development of human society. An attractive and promising method is the utilization of CO_2 as an abundant, low-cost, and renewable C1 resource to produce high value-added chemicals [1–5]. The CO_2 cycloaddition reaction has elicited widespread attention because the reaction is 100% atom-economic [6]. In addition, the produced cyclic carbonates have extensive potential applications as polar aprotic solvents, electrolytes for lithium-ion cells and batteries, and intermediates [7].

To date, a large number of homogeneous and heterogeneous catalysts have been used for the CO_2 cycloaddition reaction, including ionic liquids (ILs) [8–11], metal complexes [12–15], metal-organic frameworks (MOFs) [16–21], and porous organic polymers (POPs) [1–3,6,22–26]. Some strategies have been reported for homogeneous catalysts that catalyze the CO_2 cycloaddition reaction, but these materials still face the issues of effective adsorption and catalyst recycling [27]. Additionally, metal catalysts can significantly improve catalytic activity for the CO_2 cycloaddition reaction. Jiang et al. [28] developed a strategy to confine imidazolium-based poly(ionic liquid)s (denoted as polyILs) in the

MOF material MIL-101 via in situ polymerization of encapsulated monomers. The resultant composite polyILs@MIL-101 with a large specific surface area (2462 m^2 g^{-1}) exhibited good CO_2 capture and conversion capability at atmospheric pressure. However, the metal leaching and leftovers cause potential environmental pollution. Thus, developing effective and eco-friendly heterogeneous catalysts is necessary. The specific surface area and ionic content are important factors for the catalytic activity of porous materials. The poly(ionic liquid)s typically synthesized by free radical polymerization can have high ionic content, but they are mostly non-porous or low specific surface area materials. For example, Gai et al. [29] synthesized a new series of PIL-based copolymers through the free radical polymerization of ionic monomer and ethylene glycol dimethacrylate. The ionic content of PIL-4 reached up to 1.25 mmol g^{-1} and the specific surface area was only 1.97 m^2 g^{-1}. PIL-4 catalyzed CO_2 with epichlorohydrin into cyclic carbonate with 99% yield at 1 MPa CO_2, 100 °C in 12 h. In addition, Yavuz et al. [30] reported an imidazolinium-based catalyst produced by a one-pot reaction of terephthalaldehyde and ammonium chloride; the obtained catalyst COP-222 had high ionic content (4.05 mmol g^{-1}) and a small specific surface area (21 m^2 g^{-1}). COP-222 catalyzed epichlorohydrin with CO_2 into cyclic carbonates with a 99% yield at 0.1 MPa CO_2, 100 °C in 24 h. The high pressure and long reaction time were needed due to the small specific surface area of catalysts.

The low-cost hypercrosslinked polymers (HCPs) are promising candidate materials for CO_2 capture and conversion due to their exceptional advantages of large specific surface area and mild synthesis conditions. However, nonionic HCPs have few active functionalized sites, limiting their further application to the conversion of CO_2. Therefore, the ILs were inserted into the porous HCPs through post-functionalization strategies to obtain HIPs, which combine the advantages of HCPs and ILs. Therefore, the HIPs are widely used for CO_2 and conversion, adsorption of organic pollutants [31], and separation of bioactive molecules [32], etc. The large specific surface area and high microporosity of HCPs are efficient for CO_2 capture, and ILs can provide the catalytic active site for the conversion of CO_2. HIPs are synthesized mainly through the crosslinking of ionic and neutral monomers, in situ generations of ionic sites in the hypercrosslinked process, and post-functionalization strategies. Gai et al. [33] reported a strategy for synthesizing a series of novel HIPs via the Friedel–Crafts reaction of 2-phenylimidazole with α,α′-dichloro-p-xylene (DCX). The best active catalyst HP-[BZPhIm]Cl-DCX-1 has a large specific surface area (763 m^2 g^{-1}) and moderate IL content (0.762 mmol g^{-1}). It can convert epichlorohydrin into cyclic carbonates with 99% yield and 98% selectivity at 120 °C, 0.1 MPa CO_2 in 11 h. At present, there are few reports on the strategy of synthesizing HIPs from HCPs. Zhang et al. [34] developed a series of imidazolium-salt-modified porous HIPs through Friedel–Crafts alkylation and quaternization. The dichloroethane was used as crosslinker and solvent to construct the skeleton of HCPs containing methyl chloride, which further reacted with N-methylimidazole to form HIPs; the specific surface area and ionic content of as-prepared POM3-IM were 575 m^2 g^{-1} and 1.01 mmol g^{-1}, respectively. The resultant catalyst exhibited an 89% yield for the conversion of styrene oxide into cyclic carbonates at 120 °C for 12 h under 1 MPa CO_2. Although the aforementioned porous catalysts exhibited high catalytic yields for the cycloaddition of CO_2 with epoxides, they require harsh reaction conditions (high pressure or longer reaction time at low pressure). The primary reason is that the specific surface area and ionic content of HIPs are contradictory during the preparation process, resulting in HIPs either with a large specific surface area but excessively low ionic content or high ionic content but excessively small specific surface area. Therefore, the development of a new strategy for synthesizing HIP catalysts with high ionic content and large specific surface area is imminent.

In the current work, we developed a new strategy for synthesizing HIPs with high ionic content and large specific surface area from HCPs through addition reaction and quaternization. The synthesis route of [HCP-CH_2-Im][Cl]-X is shown in Scheme 1. In the first step, the HCP skeleton was constructed through the Friedel-Crafts alkylation reaction of diphenyl. In the second step, the prepared HCP reacts with allyl chloride to produce HCPs

with chloromethyl groups, and the addition reaction conditions (mass ratio of allyl chloride to HCP, mass ratio of H_2SO_4/HCP, reaction time, and temperature) were changed to adjust the chloromethyl content and specific surface area of HCPs. Finally, a series of imidazolium-based HIPs was prepared through quaternization with methylimidazole. The obtained [HCP-CH_2-Im][Cl]-X with high ionic content and large specific surface area catalyzed cycloaddition of CO_2 with epoxides; the reaction conditions (dosage of catalyst, reaction temperature, and reaction time) were systematically studied to obtain the optimal reaction conditions. Additionally, a range of epoxides with important industrial applications was tested to determine the universality of [HCP-CH_2-Im][Cl]-X for CO_2 cycloaddition reaction. The [HCP-CH_2-Im][Cl]-X was reused for several recycling to investigate the reusability of the catalyst. In conclusion, the HIPs with high ionic content and large specific surface area were synthesized for CO_2 cycloaddition at atmospheric pressure in a short reaction. In addition, we found that the coordination of ionic content and specific surface area is a crucial factor to achieve high catalytic activity.

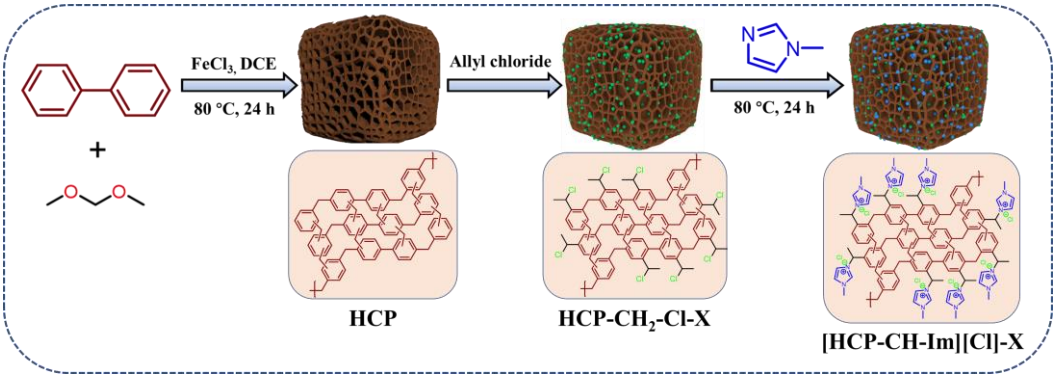

Scheme 1. Preparation of imidazolium-based hypercrosslinked ionic polymer [HCP-CH_2-Im][Cl]-X (X: different reaction conditions).

2. Results and Discussion

2.1. Influences of Addition Reaction Conditions on Chloromethyl Content and Specific Surface Area

The HCP skeleton was constructed through the Friedel–Crafts alkylation reaction of diphenyl and FDA; the specific surface area is 1153 m^2 g^{-1}. Although the specific surface areas will gradually decrease during the addition reaction and quaternization processes, the high specific surface area of HCP will provide a favorable guarantee for obtaining HIPs with high specific surface area. The addition reaction was carried out with active hydrogen on the benzene ring in the HCP skeleton by using allyl chloride as the chlorine source to produce a series of HCPs containing chloromethyl group, denoted as HCP-CH_2-Cl-X.

To obtain HCP-CH_2-Cl-X with high chloromethyl content and larger specific surface area, the influences of addition reaction conditions, including the mass ratio of allyl chloride to HCP, the mass ratio of H_2SO_4 to HCP, reaction time and temperature on chloromethyl content, and specific surface area were investigated. As shown in Figure 1a and Table S1, the effect of the mass ratio of allyl chloride to HCP was discussed. The results show that the chloromethyl content reaches the maximum (3.1 mmol g^{-1}) when the mass ratio of allyl chloride to HCP was increased to 5. However, when the mass ratio of allyl chloride to HCP increased from 5 to 9, the chloromethyl content decreased to 2.3 mmol g^{-1} because the excess allyl chloride causes the dilution of catalyst (H_2SO_4). Furthermore, with the increase of the mass ratio of allyl chloride to HCP, the specific surface areas constantly decreased due to the pore being occupied by the grafted chloromethyl. Then, on this basis, other addition reaction conditions were further studied.

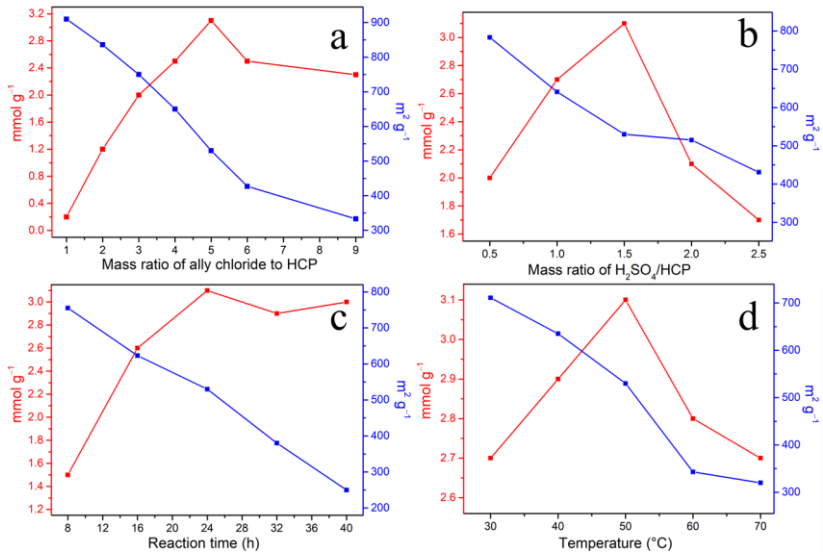

Figure 1. Effects of reaction conditions on specific surface area and content of the chloromethyl group of HCP-CH_2-Cl: (**a**) mass ratio of ally chloride to HCP, mass ratio of H_2SO_4/HCP = 1.5, 50 °C, 24 h; (**b**) mass ratio of H_2SO_4/HCP, mass ratio of ally chloride to HCP = 5, 50 °C, 24 h; (**c**) reaction time, mass ratio of ally chloride to HCP = 5, mass ratio of H_2SO_4/HCP = 1.5, 50 °C; (**d**) reaction temperature, mass ratio of ally chloride to HCP = 5, mass ratio of H_2SO_4/HCP = 1.5, 24 h.

The experimental results (Figure 1b and Table S2) show that when increasing the mass ratio of H_2SO_4/HCP from 0.5 to 1.5, a positive effect was achieved on the chloromethyl content of HCP-CH_2-Cl-X (2.0–3.1 mmol g^{-1}). However, when the mass ratio of H_2SO_4/HCP increased to 2.5, the chloromethyl contents decreased to 1.7 mmol g^{-1} because the excessive sulfuric acid generated more sulfonation reactions of the benzene ring of HCP, resulting in the passivation of the benzene ring and decreasing the chloromethyl content [35]. In addition, the specific surface area of HCP-CH_2-Cl-X decreased from 783 m^2 g^{-1} to 530 m^2 g^{-1} when the mass ratio of H_2SO_4/HCP increased from 0.5 to 1.5, which was attributed to the numerous pores that were occupied by the grafted chloromethyl group. With the increase of the mass ratio of H_2SO_4/HCP 2.5, the specific surface area was further decreased due to the pores that were occupied after sulfonation.

The results presented in Figure 1c and Table S3 show that a reaction time of 24 h is appropriate, and the highest chloromethyl content (3.1 mmol g^{-1}) was obtained. However, due to the side reaction of allyl chloride carbonization, the specific surface area was significantly reduced from 755 m^2 g^{-1} to 250 m^2 g^{-1} when the reaction time was prolonged. The effect of the reaction temperatures on the chloromethyl content and specific surface area of HCP-CH_2-Cl-X are shown in Figure 1d and Table S4. When the reaction temperature increased from 30 °C to 50 °C, the chloromethyl content gradually increased. However, the grafting amount of chloromethyl exhibited a downward trend when the temperature was higher than 50 °C because the addition reaction is exothermic. Furthermore, the specific surface area of HCP-CH_2-Cl-X was reduced when increasing the reaction temperature. The reason for this phenomenon is similar to that for the change in reaction time. The optimal addition reaction conditions were identified as follows: the mass ratio of allyl chloride to HCP (5), the mass ratio of H_2SO_4/HCP (1.5), reaction time (24 h), and temperature (50 °C); the chloromethyl content and specific surface area of HCP-CH_2-Cl-1 can reach 2.1 mmol g^{-1} and 385 m^2 g^{-1}, respectively. The HCP-CH_2-Cl-X with high chloromethyl content was obtained for the following reasons: (1) the benzene ring in the HCP framework contains abundant active sites for addition reaction; (2) the active hydrogens have been fully utilized under the optimal reaction conditions. Additionally, the HCP-CH_2-Cl-X with a large specific surface area or high chloromethyl content was selected for further quaternization reaction, denoted by HCP-CH_2-Cl-1–7. The synthesis conditions of HCP-CH_2-Cl-1–7 are shown in Table S5.

2.2. The Effects of Ionic Content and Specific Surface Area on Catalytic Activity

The corresponding HCP-CH_2-Cl-X reacted with methylimidazole to produce various HIPs ([HCP-CH_2-Im][Cl]-X) with different ionic content and specific surface area. The catalyst [HCP-CH_2-Im][Cl]-X was used to catalyze the cycloaddition reaction of CO_2 with styrene epoxide (SO) at 140 °C, 0.1 MPa in 4 h. As indicated in Table 1, [HCP-CH_2-Im][Cl]-X can effectively catalyze the cycloaddition of CO_2 with SO, and the selectivity of all the catalysts is beyond 99%. The production of styrene carbonate was negligible by using the nonionic HCP (entry 1, 5%) and HCP-CH_2-Cl-1 (entry 2, 7%) as catalysts. The catalysts with low ionic content and small specific surface area exhibited worse yields (entries 5, 7, and 9: 74%, 72%, and 72% yields, respectively). The higher yields were achieved for catalysts with low ionic content and large specific surface area under identical reaction conditions (entries 4, 6, and 8: 89%, 88%, and 84% yields, respectively). The comparison of entry 8 with entry 7 shows that the larger specific surface area (406 m^2 g^{-1} versus 183 m^2 g^{-1}) presented a higher yield (84% versus 72%) when the catalysts with the same ionic content because of the larger specific surface area can concentrate more CO_2 molecule. Entry 3 and entry 5 show that when the specific surface area of the catalysts is nearly the same, the yield of catalysts with higher ionic content is higher (95% versus 74%). In addition, the catalyst with higher ionic content (entry 7, 1.65 mmol g^{-1}) but a tiny specific surface area (183 m^2 g^{-1}) exhibited lower yield (72%) than the catalysts with lower ionic content (entries 4, 5, and 6: 0.99, 0.48, and 0.85 mmol g^{-1}, respectively) but a larger specific surface area (510, 386, and 503 m^2 g^{-1}, respectively) under identical reaction conditions. Notably, the catalyst [HCP-CH_2-Im][Cl]-1 with the highest ionic content and higher specific surface area has the highest yield of 95% (entry 3). The experimental results indicated that catalysts with excessively low ionic content or small specific surface area are not conducive to the CO_2 cycloaddition reaction; the high catalytic activity requires high ionic content, large specific surface area, and the coordination of them to achieve efficient catalysis. The catalytic activity and characterization of the catalyst [HCP-CH_2-Im][Cl]-1 were further studied.

Table 1. Cycloaddition of CO_2 with styrene oxide.

Entry	Sample [a]	IL Content [b] (mmol g^{-1})	S_{BET} [c] (m^2 g^{-1})	Yield [d] (%)	Sel. [d] (%)
1	HCP	-	1153	5	99
2	HCP-CH_2-Cl-1	-	530	7	99
3	[HCP-CH_2-Im][Cl]-1	2.10	385	95	>99
4	[HCP-CH_2-Im][Cl]-2	0.99	510	89	>99
5	[HCP-CH_2-Im][Cl]-3	0.48	386	74	99
6	[HCP-CH_2-Im][Cl]-4	0.85	503	88	>99
7	[HCP-CH_2-Im][Cl]-5	1.65	183	72	99
8	[HCP-CH_2-Im][Cl]-6	1.81	406	84	>99
9	[HCP-CH_2-Im][Cl]-7	1.26	295	72	99

[a] Reaction condition: 5 mmol styrene oxide, catalyst (25 wt%), CO_2 (0.1 MPa), 140 °C, 4 h. [b] IL content calculated by elemental analysis. [c] BET specific surface area. [d] Yield and selectivity were determined by 1H NMR.

2.3. Characterization of Polymers

The Fourier transform infrared (FTIR) spectra of HCP (a), HCP-CH_2-Cl-1 (b), and [HCP-CH_2-Im][Cl]-1 (c) are shown in Figure 2. The (b) exhibited a characteristic peak at 617 cm^{-1}, which belonged to the vibrative absorption of C-Cl [36]. The absorption of C-Cl weakened and the characteristic peak of the imidazolium ring appeared at 1598 cm^{-1} and 1167 cm^{-1} after quaternization, which belonged to the imidazolium ring stretching of C=N and C-N, respectively [1,6,37]. The preceding results indicated that imidazolium-based HIPs were successfully prepared. The thermogravimetric analysis (TGA) curves of HCP,

HCP-CH_2-Cl-1, and [HCP-CH_2-Im][Cl]-1 in Figure 3a illustrate that the catalysts exhibited favorable thermal stability. In particular, the weight loss of HCP, HCP-CH_2-Cl-1, and [HCP-CH_2-Im][Cl]-1 started at 324 °C, 360 °C, and 236 °C, respectively, which are considerably higher than the reaction temperature.

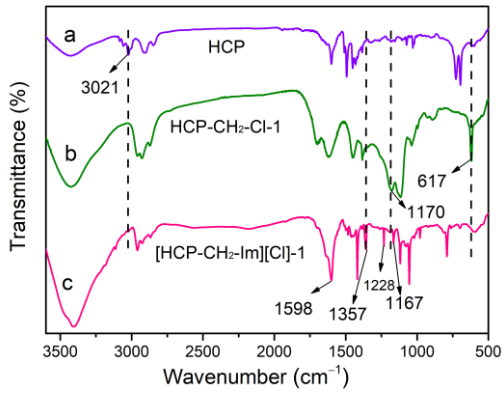

Figure 2. FT-IR spectra of (**a**) HCP, (**b**) HCP-CH_2-Cl-1, and (**c**) [HCP-CH_2-Im][Cl]-1.

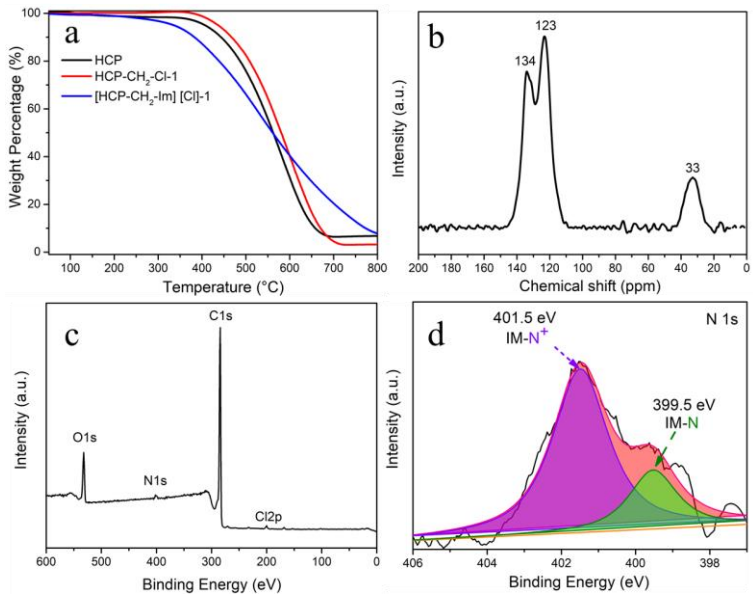

Figure 3. (**a**) TGA curves of HCP, HCP-CH_2-Cl-1, and [HCP-CH_2-Im][Cl]-1, (**b**) ^{13}C CP/MAS NMR spectrum of [HCP-CH_2-Im][Cl]-1, (**c**) survey scan, and (**d**) N 1 s XPS spectra of [HCP-CH_2-Im][Cl]-1.

The [HCP-CH_2-Im][Cl]-1 sample was further characterized via solid-state ^{13}C NMR and X-ray photoelectron spectroscopy (XPS). As shown in Figure 3b, the signals at 134 ppm and 123 ppm belonged to the imidazole ring and aromatic carbons of the benzene ring, respectively. Meanwhile, the peak at 33 ppm originated from the methylene carbon formed via Friedel–Crafts reaction [34,38,39]. The survey scan XPS spectrum produced signals at 532.3, 401.6, 284.0, 270.4, and 199.8 eV, which belonged to the element species of C 1s, O 1s, N 1s, Br 3s, and Cl 2p (Figure 3c), respectively. The XPS of the N 1s of [HCP-CH_2-Im][Cl]-1 (Figure 3d) shows two peaks at 399.5 eV and 401.5 eV, which are assigned to the nonionic N atoms and imidazolinium cations, respectively [40,41]. The preceding results indicate that imidazolium was successfully grafted onto the backbone of the HIP.

Scanning electron microscopy (SEM) images (Figure 4a,b,e,f,i,j) showed that the polymers were composed of anomalistic nanoparticles at the micrometer level. Elemental mapping images (Figure 4c,d,g,h,k,l) showed that Cl and N were dispersed throughout the polymer skeleton, indicating that ionic sites were uniformly dispersed in the polymer

skeleton. The Cl content was significantly increased after the addition reaction. Meanwhile, N content was significantly increased and Cl content remained unchanged after quaternization. These results further prove that the successful preparation of HIPs occurred. In addition, the aforementioned morphology of [HCP-CH_2-Im][Cl]-1 was illustrated through transmission electron microscopy images (Figure 5). X-ray diffraction patterns indicate that HCPs and HIPs were amorphous (Figure S1).

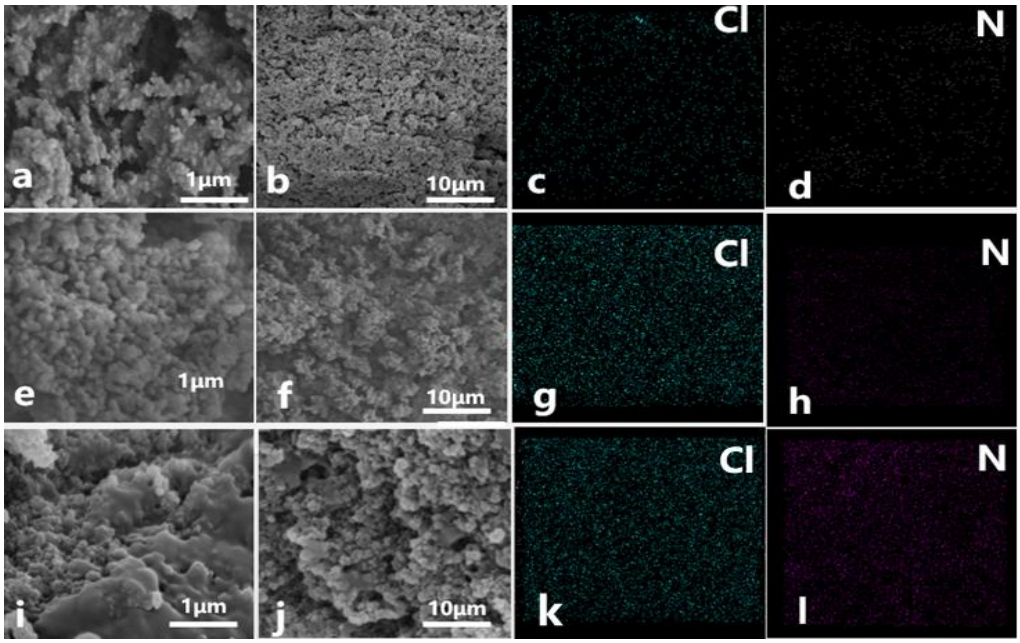

Figure 4. SEM images and elemental (N and Cl) mapping images of HCP (**a**–**d**), HCP-CH_2-Cl-1 (**e**–**h**), and [HCP-CH_2-Im][Cl]-1 (**i**–**l**).

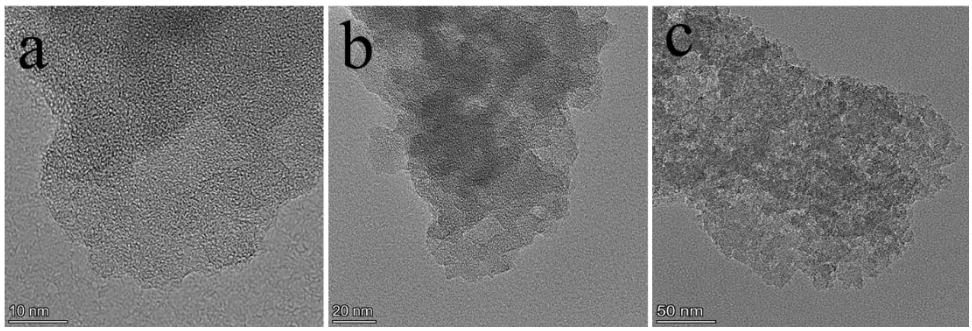

Figure 5. TEM images of [HCP-CH_2-Im][Cl]-1 (**a**) 10 nm; (**b**) 20 nm; (**c**) 50 nm).

The porosity of [HCP-CH_2-Im][Cl]-X was studied through N_2 adsorption experiments. As shown in Figure 6a, the prepared [HCP-CH2-Im][Cl]-X presents typical Type IV isotherms [42] and the adsorption curve rose faster in the low-pressure area, which indicates that the material contained a certain number of microporous structures, which was conducive to CO_2 concentration [43]. Furthermore, the pore size distribution diagram was calculated using the nonlocal density function in Figure 6b; the pores of the polymers were mostly concentrated at approximately 1 nm to 6 nm and are microporous/mesoporous structures. The existence of a mesoporous structure was beneficial for mass transfer and accelerated the reaction rate [44]. The morphological properties of [HCP-CH_2-Im][Cl]-X are summarized in Table S6 in accordance with the N_2 isotherm; the [HCP-CH_2-Im][Cl]-X is primarily composed of microporous structures and a small number of mesoporous structures. Figure S2a shows that the CO_2 isotherms of [HCP-CH_2-Im][Cl]-1 have relative pressure

ranging from 0 bar to 1.0 bar at 273 K and 298 K. The CO_2 uptakes of [HCP-CH_2-Im][Cl]-1 are 1.79 mmol g^{-1} (273 K) and 1.20 mmol g^{-1} (298 K). Moreover, Figure S2b illustrates that CO_2 uptakes exhibited almost no decrease after adsorption-desorption was run five times, demonstrating excellent reusability.

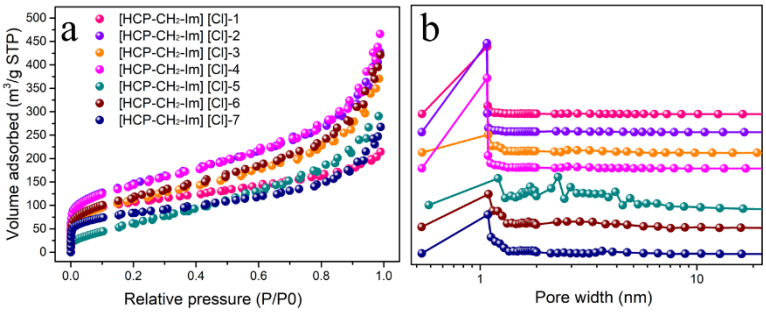

Figure 6. (**a**) N_2 adsorption-desorption isotherms, (**b**) pore size distribution of [HCP-CH_2-Im][Cl]-X.

2.4. Optimization of Cycloaddition Reaction Conditions and the Universality of Catalysts

The catalytic activity of [HCP-CH_2-Im][Cl]-1 was further studied to obtain the optimal reaction conditions for the cycloaddition of CO_2 with epoxides. As shown in Figure 7, the effects of temperature, mass ratio of the catalyst to SO, and reaction time on the catalytic activity of [HCP-CH_2-Im][Cl]-1 were investigated by using SO as substrate. The catalyst [HCP-CH_2-Im][Cl]-1 exhibited high selectivity (99%) under all reaction conditions. In Figure 7a, the reaction temperature exerted a remarkable effect on the yields for the cycloaddition reaction. When the reaction temperature was increased within the range of 50 to 140 °C, the yield of cyclic carbonate increased from 5% to 99%, and then it became stable when the temperature was further increased to 150 °C. When the mass ratio of the catalyst to SO increased from 0 wt% to 25 wt% (Figure 7b), carbonate yield constantly increased from 1% to 99%. Figure 7c shows the effect of reaction time at 140 °C, 25 wt% mass ratio of the catalyst to SO, and 0.1 MPa CO_2 on catalytic activity. Cyclic carbonate yield exhibited a gradual increase from 1 h to 5 h (yield from 62% to 99%), and remained unchanged when the reaction time was increased to 6 h. [HCP-CH_2-Im][Cl]-1 exhibited 99% yield and 99% selectivity for the cycloaddition of CO_2 with SO under optimal reaction conditions (0.1 MPa CO_2, 140 °C, 25 wt% catalysts, 5 h).

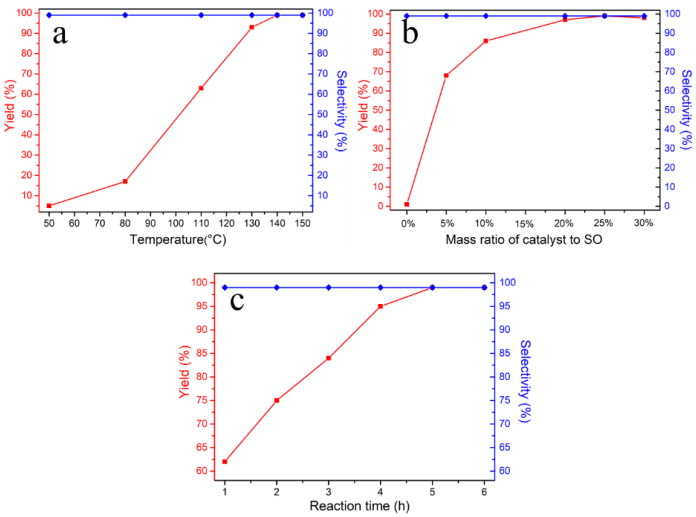

Figure 7. Effect of yield and selectivity as a function of (**a**) temperature, styrene oxide (5 mmol), 0.1 MPa CO_2, 5 h, [HCP-CH_2-Im][Cl]-1 (25 wt%); (**b**) mass ratio of catalyst to SO, styrene oxide (5 mmol), 0.1 MPa CO_2, 140 °C, 5 h; (**c**) reaction time, styrene oxide (5 mmol), 0.1 MPa CO_2, 140 °C, [HCP-CH_2-Im][Cl]-1 (25 wt%).

A range of epoxides with important industrial applications was tested to determine the universality of [HCP-CH_2-Im][Cl]-1 for CO_2 cycloaddition reaction. All the examined substrates exhibited excellent yield and selectivity under optimal conditions as summarized in Table 2. The yields of the products from propylene oxide, epichlorohydrin, and epibromohydrin reached 99% within 4 h (entries 1–3). The catalytic activity of the catalyst [HCP-CH_2-Im][Cl]-1 for SO was further studied at lower temperatures; it can be found that excellent catalytic yields (entry 4) were achieved by slightly extending the reaction time at lower temperatures. Moreover, although less reactive substrates with long chains and oxymethylene moiety required a longer reaction time, excellent yields were still obtained at 140 °C, 0.1 MPa CO_2 (6 h, 91–99%, entries 5–8). The experimental results demonstrated that the catalyst [HCP-CH_2-Im][Cl]-1 exhibited excellent catalytic activity for similar substrates. The reaction time of the [HCP-CH_2-Im][Cl]-1 catalyst was compared with those of recently reported heterogeneous porous catalysts for the cycloaddition of CO_2 with SO (Table S7). By contrast, [HCP-CH_2-Im][Cl]-1 required a shorter reaction time than the same type of catalysts under the same reaction conditions.

Table 2. Cycloaddition of CO_2 to various epoxides catalyzed by [HCP-CH_2-Im][Cl]-1.

Entry [A]	Substrate	Product	Time (h)	Yield [B] (%)	Sel. [B] (%)
1			4	99	99
2			4	99	99
3	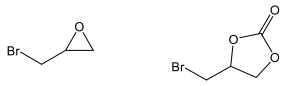		4	99	>99
4	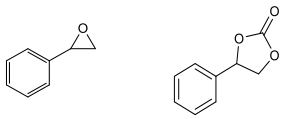		5 8 20	99 94 (120 °C) 93 (100 °C)	99 >99 99
5	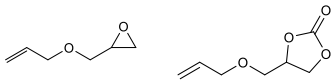		6	92	>99
6	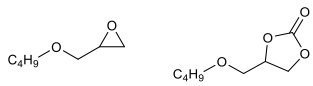		6	91	>99
7 [C]	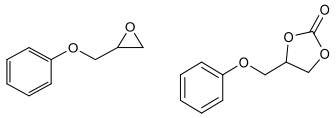		6	95 [C]	-
8	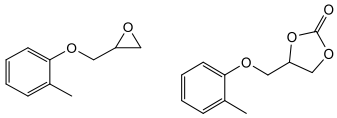		6	99	99

[a] Reaction condition: 5 mmol epoxides, [HCP-CH_2-Im][Cl]-1 (25 wt%), CO_2 (0.1 MPa), 140 °C. [b] Yield and selectivity were determined by ^{1}H NMR. [c] Isolate yield by recrystallization.

2.5. Reusability of Catalysts

The reusability of catalysts is an important factor in economic and industrial applications. To investigate the reusability of the HIP catalyst [HCP-CH_2-Im][Cl]-1, the SO was used as the substrate for cycloaddition reaction under optimal reaction conditions. After the reaction, ethyl acetate was added to separate the cyclic carbonates from the catalyst [HCP-CH_2-Im][Cl]-1 via filtration. Then the catalyst [HCP-CH_2-Im][Cl]-1 was dried under vacuum and applied in the next run. As shown in Figure 8a, the catalyst was run six

times and its catalytic activity did not drop significantly (90–99% yield and 99% selectivity). The slight decrease in catalytic activity due to catalyst loss during the separation process demonstrates the excellent reusability of the [HCP-CH_2-Im][Cl]-1. The stability of the catalyst [HCP-CH_2-Im][Cl]-1 after six run times was studied via SEM, FTIR, and TGA. The recycled catalyst [HCP-CH_2-Im][Cl]-1 showed a dense pore structure in the SEM image shown in Figure 8b. Furthermore, the characteristic peak of recycled catalyst presented no evident change in contrast with the FTIR spectrum of the fresh catalyst, and the newly emerged characteristic peaks 1790 cm^{-1} and 1672 cm^{-1} belong to cyclic carbonate (Figure 8c). As shown in Figure 8d, the stability of the catalyst was further examined through TGA. The thermal stability of the reused [HCP-CH_2-Im][Cl]-1 catalyst after six run times was as good as that of the fresh catalyst. These results proved that the recycled catalyst [HCP-CH_2-Im][Cl]-1 can meet the reaction temperature requirement.

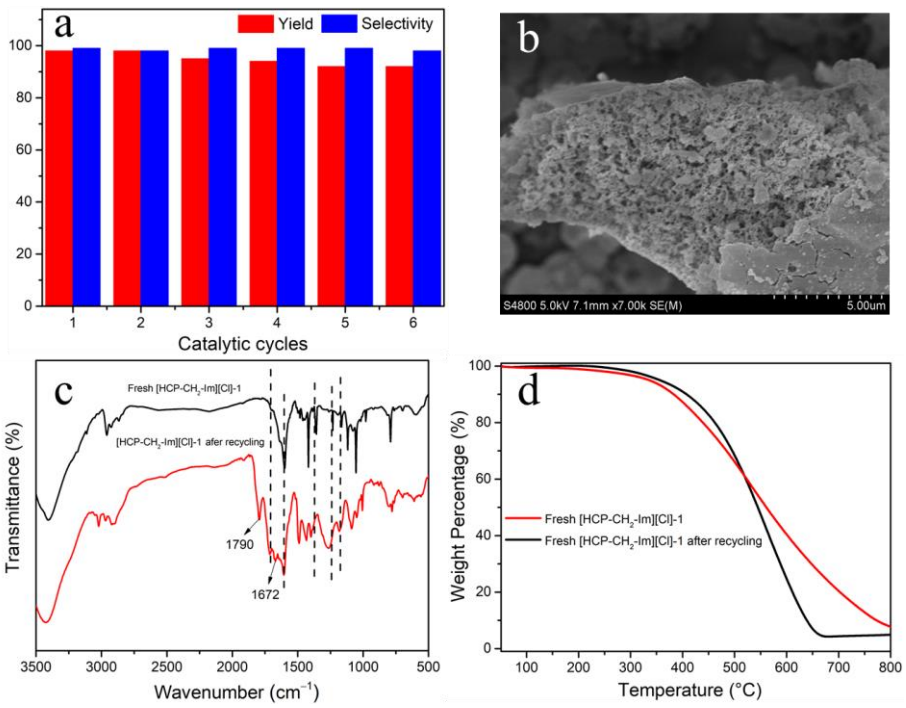

Figure 8. (**a**) Reusability of [HCP-CH_2-Im][Cl]-1 for CO_2 cycloaddition with epichlorohydrin. Reaction conditions: styrene oxide (5 mmol), CO_2 (0.1 MPa), catalyst (25 wt%), 140 °C, 5 h, (**b**) SEM image, (**c**) FT-IR spectrum, (**d**) TG curves of [HCP-CH_2-Im][Cl]-1 after having been run 6 times.

2.6. Proposed Mechanism

The proposed catalytic mechanism of [HCP-CH_2-Im][Cl]-1 in catalyzing CO_2 conversion into cyclic carbonates is illustrated in Scheme 2. In all the aforementioned steps, the step to determine the CO_2 cycloaddition rate is typically known as the epoxy ring opening step [45,46]. As shown in Scheme 2, when the epoxide entered the pores of the catalyst, the C-O bond of epoxide was activated by the interaction between the oxygen atom and imidazolium cation, accelerating the ring opening of the epoxide (Step 1) [25,47,48]. Meanwhile, the chloride anion of [HCP-CH_2-Im][Cl]-1 attacked the α-carbon atom of the epoxy ring to produce the ring opening intermediate (Step 2). Subsequently, CO_2 was adsorbed by the [HCP-CH_2-Im][Cl]-1 and inserted into the strongly nucleophilic intermediate to generate cyclic esters (Step 3). Finally, cyclic carbonates were formed through the elimination of chloride ions and the intramolecular cyclization of acyclic ester (Step 4), followed by the regeneration of the catalyst for the next run.

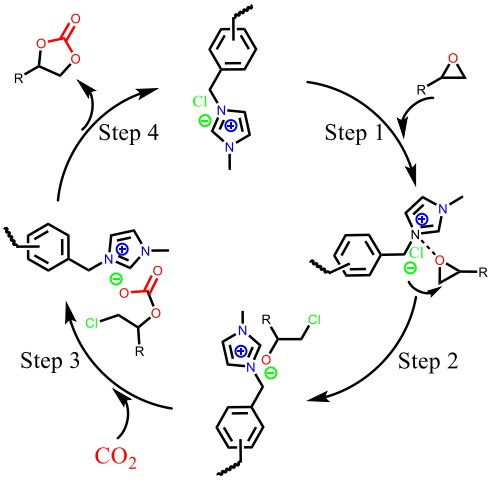

Scheme 2. Plausible mechanism for [HCP-CH_2-Im][Cl]-1 catalyzed CO_2 cycloaddition with epoxides.

3. Experimental Section

3.1. Materials

The commercial chemicals and reagents were used as received without further purification unless otherwise stated. Allyl chloride (98%), diphenyl (99%), dichloroethane (DCE, 99%), dimethoxy methane (FDA, 98%), 1-methylimidazole (99%), epichlorohydrin (AR), allyl glycidyl ether (99%), butyl glycidyl ether (98%), propylene oxide (99%), and o-Tolyl glycidyl ether (90%) were provided by Aladdin Chemical Reagent Co. LTD (Beijing, China). Sulfuric acid (98%), ferric chloride ($FeCl_3$, 98%), and ethyl acetate (EtOAc, AR) were purchased from Sinopharm Chemical Reagent Co. LTD. Styrene oxide (98%), glycidyl phenyl ether (99%), and 1,2-ethylene dibromide (98%) were purchased from Energy Chemical Reagent Co., Ltd. (Shanghai, China).

3.2. Characterization

The IR spectra were obtained using an FT-IR (4000~400 cm^{-1}) spectrometer (Nicolet Nexus FT-IR spectrometer (Madison, WI USA) at 4 cm^{-1} resolution and 32 scans. NMR spectra were acquired in $CDCl_3$ on a Bruker AVANCE III 500 MHz spectrometer (Zurich, Switzerland) for ^{1}H NMR; the particular NMR spectra can be found in the Supplementary Material (Figures S3–S10). ^{13}C CP/MAS NMR spectra were measured on an Agilent-NMR-VnmrS 600 (Palo Alto, CA, USA). Thermogravimetric analysis (TGA-50H, Shimadzu, Kyoto, Japan) of the samples was carried out: they were heated from 50 to 800 °C at ramp 10 °C/min under Ar gas flow. Brunauer–Emmett–Teller (BET) pore volumes and surface areas were recorded with N_2 adsorption at 77 K by using JWGB (JW-DEL 200 (Beijing, China). The crystal structure of the samples was examined by X-ray diffraction (XRD) on SmartLa. CHNS elemental analysis was performed on the Vario EL Cube. Field emission scanning electron microscope (FESEM; Hitachi S-4800, accelerated voltage: 5 kV (Tokyo, Japan) was used to observe the morphology. Transmission electron microscope (TEM) images of the samples were examined by Hitachi H-7650 (Tokyo, Japan). X-ray photoelectron spectroscopy (XPS) of the [HCP-CH_2-Im][Cl]-1 was determined by Thermo Fisher Scientific K-alpha$^+$ (Waltham, MA, USA) equipped with Al K radiation (1486.68 eV).

3.3. Synthesis of HCP

A mixture of biphenyl (0.02 mol, 3.084 g) and FDA (5.3 mL) in DCE (50 mL) was stirred for 10 min at room temperature. $FeCl_3$ (9.732 g, 0.06 mol) was then added and the mixture was heated to 80 °C for 24 h. The resultant polymers were filtered and washed with methanol, and further purified for 24 h via Soxhlet extractions with methanol as solvent. The obtained HCP was vacuum-dried at 80 °C for 24 h.

3.4. Synthesis of HCP-CH_2-Cl-X

A mixture of HCP (1 g) and ethyl acetate (40 mL) was swelled at 60 °C and in 2 h. Then the mixture was cooled to room temperature, and allyl chloride (5.3 mL) was added to the mixture. The ethyl acetate (10 mL) and sulfuric acid (1.5 g) were added to the mixture by using a constant pressure separatory funnel, and the reaction was carried out at 50 °C for 24 h. After the reaction, the products were washed with ethyl acetate and deionized water and dried in a vacuum at 80 °C for 24 h to obtain HCP-CH_2-Cl-1. The other HCP-CH_2-Cl-X was synthesized similarly using the aforementioned procedures under different reaction conditions.

3.5. Synthesis of [HCP-CH_2-Im][Cl]-X

A mixture of the HCP-CH_2-Cl-1 (1 g) and ethyl acetate was heated to 50 °C for 2 h for the swelling of the polymers and then 1-methylimidazole (0.02 mol, 1.64 g) was added to the mixture; the reaction was heated to 80 °C for 24 h. The resultant polymers were washed with ethyl acetate and further dried under vacuum at 80 °C for 24 h. The other [HCP-CH_2-Im][Cl]-X was synthesized following the same procedure.

3.6. General Catalytic Procedure for CO_2 Cycloaddition to Epoxides

In a typical run, styrene oxide (SO, 5 mmol) and [HCP-CH_2-Im][Cl]-1 (25 wt%) were charged into a high-pressure stainless steel autoclave (Figure S11), which was pressured with CO_2 (0.1 MPa), and the reactant was heated to 140 °C for 5 h. After the reaction and cooling to room temperature, the remaining CO_2 was released slowly. The product was diluted with ethyl acetate and the liquid phase was separated via filtration. The ethylene dibromide (0.5 mmol, 36 μL) was added as the internal standard after the rotary evaporation of ethyl acetate. The yield and selectivity were analyzed via ^{1}H NMR.

4. Conclusions

A new strategy for synthesizing hypercrosslinked imidazolium-based ionic polymers with high ionic content and higher specific surface area from porous HCPs was developed through addition reaction and quaternization. The specific surface area and ionic content of HIPs could be adjusted by optimizing addition reaction conditions (the mass ratio of allyl chloride to HCP, reaction temperature, the ratio of H_2SO_4/HCP, and reaction time). FT-IR, solid-state ^{13}C NMR, XPS, and SEM mapping demonstrated that the HIPs were successfully prepared. The obtained HIP [HCP-CH_2-Im][Cl]-1 with high ionic content and higher specific surface area not only possessed good CO_2 uptake but also exhibited outstanding catalytic yields for most epoxy substrates (99% selectivity and 91–99% yield) at atmospheric pressure in a shorter reaction time (4–6 h) without cocatalyst, solvent, and additive. In addition, the catalyst [HCP-CH_2-Im][Cl]-1 demonstrated excellent reusability and stability after six run times. The high ionic content of HIPs provides more reaction sites and high microporosity that could enrich CO_2, which contributes to the efficient conversion of CO_2 into cyclic carbonates. This work provides a new strategy to synthesize imidazolium-based HIPs with high catalytic activity from porous HCPs for the cycloaddition of CO_2 with epoxides at atmospheric pressure. Furthermore, we determined that the coordination of ionic content and specific surface area is a crucial factor for high catalytic activity for the cycloaddition of CO_2 with epoxides.

Supplementary Materials: The following are available online at https://www.mdpi.com/article/10.3390/catal12010062/s1, Figure S1: XRD patterns of HCP, HCP-CH_2-Cl-1, [HCP-CH_2-IM][Cl]-1; Figure S2: (a) CO_2 adsorption isotherms of [HCP-CH_2-Im][Cl] (1) at 273 K and 298 K, (b) recycling performance of [HCP-CH_2-Im][Cl] (1) at 273 K. Figures S3–S10: ^{1}H NMR spectra of cyclic carbonates. Table S1: The effect of mass ratio of allyl chloride/HCP on specific surface area and chloromethyl content of HCP-CH_2-Cl-X; Table S2: The effect of mass ratio of H_2SO_4/HCP on specific surface area and chloromethyl content of HCP-CH_2-Cl-X; Table S3: The effect of reaction time on specific surface area and chloromethyl content of HCP-CH_2-Cl-X; Table S4: The effect of reaction temperature on

specific surface area and chloromethyl content of HCP-CH_2-Cl-X; Table S5: The synthesis conditions of HCP-CH_2-Cl-X; Table S6: Textual properties of [HCP-CH_2-Im][Cl]-X; Table S7: Activity of porous ionic polymers in the cycloaddition of CO_2 with styrene oxide.

Author Contributions: Conceptualization, X.L. (Xu Liao), B.P. and J.L.; methodology, X.L. (Xu Liao) and B.P.; investigation, X.L. (Xu Liao); resources, X.L. (Xu Liao), B.P. and J.L.; data curation, X.L. (Xu Liao), B.P., R.M., J.H., L.K. and X.G.; writing—original draft preparation, X.L. (Xu Liao); writing—review and editing, X.L. (Xu Liao), X.L. (Xiaoyan Luo) and J.L.; visualization, X.L. (Xu Liao) and J.L.; supervision, X.L. (Xiaoyan Luo) and J.L.; project administration, J.L.; funding acquisition, J.L. All authors have read and agreed to the published version of the manuscript.

Funding: Financial support from the National Natural Science Foundation of China (21803021, 21246008) and the Natural Science Foundation of Fujian Province (2020J01065).

Data Availability Statement: The data presented in this study are available on request from the corresponding author via e-mail: linlab505@hqu.edu.cn (J.L.).

Acknowledgments: This work was supported by the National Natural Science Foundation of China (21803021, 21246008) and the Natural Science Foundation of Fujian Province (2020J01065). The authors give thanks for the support of the Instrumental Analysis Center, Huaqiao University.

Conflicts of Interest: The authors declare that they have no known competing financial interests or personal relationships that could have appeared to influence the work reported in this paper.

References

1. Jia, D.; Ma, L.; Wang, Y.; Zhang, W.; Li, J.; Zhou, Y.; Wang, J. Efficient CO_2 enrichment and fixation by engineering micropores of multifunctional hypercrosslinked ionic polymers. *Chem. Eng. J.* **2020**, *390*, 124652. [CrossRef]
2. Xie, Y.; Liang, J.; Fu, Y.; Huang, M.; Xu, X.; Wang, H.; Tu, S.; Li, J. Hypercrosslinked mesoporous poly(ionic liquid)s with high ionic density for efficient CO_2 capture and conversion into cyclic carbonates. *J. Mater. Chem. A.* **2018**, *6*, 6660–6666. [CrossRef]
3. Zhang, W.; Ma, F.; Ma, L.; Zhou, Y.; Wang, J. Imidazolium-functionalized ionic hypercrosslinked porous polymers for efficient synthesis of cyclic carbonates from simulated flue gas. *ChemSusChem* **2020**, *13*, 341–350. [CrossRef] [PubMed]
4. Liu, Q.; Wu, L.; Jackstell, R.; Beller, M. Using carbon dioxide as a building block in organic synthesis. *Nat. Commun.* **2015**, *6*, 5933. [CrossRef]
5. Ma, D.; Liu, K.; Li, J.; Shi, Z. Bifunctional metal-free porous organic framework heterogeneous catalyst for efficient CO_2 conversion under mild and cocatalyst-free conditions. *ACS Sustain. Chem. Eng.* **2018**, *6*, 15050–15055. [CrossRef]
6. Sang, Y.; Huang, J. Benzimidazole-based hyper-cross-linked poly(ionic liquid)s for efficient CO_2 capture and conversion. *Chem. Eng. J.* **2020**, *385*, 123973. [CrossRef]
7. Zhang, Y.; El-Sayed, E.M.; Su, K.; Yuan, D.; Han, Z. Facile syntheses of ionic polymers for efficient catalytic conversion of CO_2 to cyclic carbonates. *J. CO2 Util.* **2020**, *42*, 101301. [CrossRef]
8. Li, Y.D.; Cui, D.X.; Zhu, J.C.; Huang, P.; Tian, Z.; Jia, Y.Y.; Wang, P.A. Bifunctional phase-transfer catalysts for fixation of CO_2 with epoxides under ambient pressure. *Green Chem.* **2019**, *21*, 5231–5237. [CrossRef]
9. Mosteirin, N.F.; Jehanno, C.; Ruiperez, F.; Sardon, H.; Dove, A.P. Rational study of DBU salts for the CO_2 insertion into epoxides for the synthesis of cyclic carbonates. *ACS Sustain. Chem. Eng.* **2019**, *7*, 10633–10640. [CrossRef]
10. Xu, X.; Chen, C.; Guo, Z.; North, M.; Whitwood, A.C. Metal-and halide-free catalyst for the synthesis of cyclic carbonates from epoxides and carbon dioxide. *ACS Catal.* **2019**, *9*, 1895–1906.
11. Alves, M.; Grignard, B.; Mereau, R.; Jerome, C.; Tassaing, T.; Detrembleur, C. Organocatalyzed coupling of carbon dioxide with epoxides for the synthesis of cyclic carbonates: Catalyst design and mechanistic studies. *Catal. Sci. Technol.* **2017**, *7*, 2651–2684. [CrossRef]
12. Peng, J.; Yang, H.J.; Geng, Y.; Wei, Z.; Wang, L.; Guo, C.Y. Novel, recyclable supramolecular metal complexes for the synthesis of cyclic carbonates from epoxides and CO_2 under solvent-free conditions. *J. CO2 Util.* **2017**, *17*, 243–255. [CrossRef]
13. Deacy, A.C.; Kilpatrick, A.F.R.; Regoutz, A.; Williams, C.K. Understanding metal synergy in heterodinuclear catalysts for the copolymerization of CO_2 and epoxides. *Nat. Chem.* **2020**, *12*, 372–380. [CrossRef] [PubMed]
14. Andrea, K.A.; Butler, E.D.; Brown, T.R.; Anderson, T.S.; Jagota, D.; Rose, C.; Lee, E.M.; Goulding, S.D.; Murphy, J.N.; Kerton, F.M.; et al. Iron complexes for cyclic carbonate and polycarbonate formation: Selectivity control from ligand design and metal-center geometry. *Inorg. Chem.* **2019**, *58*, 11231–11240. [CrossRef]
15. Yang, H.Q.; Chen, Z.X. Theoretical investigation on conversion of CO_2 with epoxides to cyclic carbonates by bifunctional metal-salen complexes bearing ionic liquid substsituents. *Mol. Catal.* **2021**, *511*, 111733. [CrossRef]
16. Benedito, A.; Acarreta, E.; Gimenez, E. A highly efficient MOF catalyst systems for CO_2 conversion to bis-cyclic carbonates as building blocks for NIPHUs (non-isocyanate polyhydroxyurethanes) synthesis. *Catalysts* **2021**, *11*, 628. [CrossRef]
17. Akimana, E.; Wang, J.; Likhanova, N.V.; Chaemchuen, S.; Verpoort, F. MIL-101(Cr) for CO_2 conversion into cyclic carbonates under solvent and Co-catalyst free mild reaction conditions. *Catalysts* **2020**, *10*, 453. [CrossRef]

18. Liang, L.; Liu, C.; Jiang, F.; Chen, Q.; Zhang, L.; Xue, H.; Jiang, H.L.; Qian, J.; Yuan, D.; Hong, M. Carbon dioxide capture and conversion by an acid-base resistant metal-organic framework. *Nat. Commun.* **2017**, *8*, 1233. [CrossRef]
19. Pander, M.; Janeta, M.; Bury, W. Quest for an efficient 2-in-1 MOF-based catalytic system for cycloaddition of CO_2 to epoxides under mild conditions. *ACS Appl. Mater. Interfaces* **2021**, *13*, 8344–8352. [CrossRef]
20. Abazari, R.; Sanati, S.; Morsali, A.; Kirillov, A.M.; Slawin, A.M.Z.; Carpenter-Warren, C.L. Simultaneous presence of open metal sites and amine groups on a 3D Dy(III)-metal-organic framework catalyst for mild and solvent-free conversion of CO_2 to cyclic carbonates. *Inorg. Chem.* **2021**, *60*, 2056–2067. [CrossRef]
21. Zhang, Y.; Xu, W.G.; Han, Z.B. MOF@POP core–shell architecture as synergetic catalyst for high-efficient CO_2 fixation without cocatalyst under mild conditions. *J. CO2 Util.* **2021**, *46*, 101463. [CrossRef]
22. Yu, W.; Gu, S.; Fu, Y.; Xiong, S.; Pan, C.; Liu, Y.; Yu, G. Carbazole-decorated covalent triazine frameworks: Novel nonmetal catalysts for carbon dioxide fixation and oxygen reduction reaction. *J. Catal.* **2018**, *362*, 1–9. [CrossRef]
23. Siewniak, A.; Forajter, A.; Szymanska, K. Mesoporous silica-supported ionic liquids as catalysts for styrene carbonate synthesis from CO_2. *Catalysts* **2020**, *10*, 1363. [CrossRef]
24. Wang, J.; Zhang, Y. Facile synthesis of N-rich porous azo-linked frameworks for selective CO_2 capture and conversion. *Catalysts* **2020**, *10*, 1363. [CrossRef]
25. Wang, X.; Dong, Q.; Xu, Z.; Wu, Y.; Gao, D.; Xu, Y.; Ye, C.; Wen, Y.; Liu, A.; Long, Z.; et al. Hierarchically nanoporous copolymer with built-in carbene-CO_2 adducts as halogen-free heterogeneous organocatalyst towards cycloaddition of carbon dioxide into carbonates. *Chem. Eng. J.* **2021**, *403*, 126460. [CrossRef]
26. Li, Y.; Zhang, J.; Zuo, K.; Li, Z.; Wang, Y.; Hu, H.; Zeng, C.; Xu, H.; Wang, B.; Gap, Y. Covalent organic frameworks for simultaneous CO_2 capture and selective catalytic transformation. *Catalysts* **2021**, *11*, 1133. [CrossRef]
27. Huang, K.; Zhang, J.Y.; Liu, F.; Dai, S. Synthesis of porous polymeric catalysts for the conversion of carbon dioxide. *ACS Catal.* **2018**, *8*, 9079–9102. [CrossRef]
28. Ding, M.; Jiang, H.L. Incorporation of imidazolium-based poly(ionic liquid)s into a metal–organic framework for CO_2 capture and conversion. *ACS Catal.* **2018**, *8*, 3194–3201. [CrossRef]
29. Song, H.; Wang, Y.; Xiao, M.; Liu, L.; Liu, Y.; Liu, X.; Gi, H. Design of novel poly(ionic liquids) for the conversion of CO_2 to cyclic carbonates under mild conditions without solvent. *ACS Sustain. Chem. Eng.* **2019**, *7*, 9489–9497. [CrossRef]
30. Subramanian, S.; Oppenheim, J.; Kim, D.; Nguyen, T.; Silo, W.; Kim, B.; Goddard, W.; Yavuz, C. Catalytic non-redox carbon dioxide fixation in cyclic carbonates. *Chem* **2019**, *5*, 3232–3242. [CrossRef]
31. Shen, R.; Yan, X.; Guan, Y.J.; Zhu, W.; Li, T.; Liu, X.G.; Li, Y.; Gu, Z.G. One-pot synthesis of a highly porous anionic hypercrosslinked polymer for ultrafast adsorption of organic pollutants. *Polym. Chem.* **2018**, *9*, 4724–4732. [CrossRef]
32. Suo, X.; Huang, Y.; Li, Z.; Pan, H.; Gui, X.; Xing, H. Construction of anion-functionalized hypercrosslinked ionic porous polymers for efficient separation of bioactive molecules. *Sci. China Mater.* **2021**. [CrossRef]
33. Song, H.; Wang, Y.; Liu, Y.; Chen, L.; Feng, B.; Jin, X.; Zhou, Y.; Huang, T.; Xiao, M.; Huang, F.; et al. Conferring poly(ionic liquid)s with high surface areas for enhanced. *ACS Sustain. Chem. Eng.* **2021**, *9*, 2115–2128. [CrossRef]
34. Wang, J.; Sng, W.; Yi, G.; Zhang, Y. Imidazolium salt-modified porous hypercrosslinked polymers for synergistic CO_2 capture and conversion. *Chem. Commun.* **2015**, *51*, 12076–12079. [CrossRef] [PubMed]
35. Pei, B.; Xiang, X.; Liu, T.; Li, D.; Zhao, C.; Qiu, R.; Chen, X.; Lin, J.; Luo, X. Preparation of chloromethylated pitch-based hyper-crosslinked polymers and an immobilized acidic ionic liquid as a catalyst for the synthesis of biodiesel. *Catalysts* **2019**, *9*, 963. [CrossRef]
36. Gan, Y.; Chen, G.; Sang, Y.; Zhou, F.; Man, R.; Huang, J. Oxygen-rich hyper-cross-linked polymers with hierarchical porosity for aniline adsorption. *Chem. Eng. J.* **2019**, *368*, 29–36. [CrossRef]
37. Puthiaraj, P.; Ravi, S.; Yu, K.; Ahn, W.S. CO_2 Adsorption and conversion into cyclic carbonates over a porous $ZnBr_2$-grafted N-heterocyclic carbene-based aromatic polymer. *Appl. Catal. B Environ.* **2019**, *251*, 195–205. [CrossRef]
38. Zhang, Y.; Zhao, L.; Patra, P.K.; Hu, D.; Ying, J.Y. Colloidal poly-imidazolium salts and derivatives. *Nano Today* **2009**, *4*, 13–20. [CrossRef]
39. Li, J.; Jia, D.; Guo, Z.; Liu, Y.; Lyu, Y.; Zhou, Y.; Wang, J. Imidazolinium based porous hypercrosslinked ionic polymers for efficient CO_2 capture and fixation with epoxides. *Green Chem.* **2017**, *19*, 2675–2686. [CrossRef]
40. Chen, G.; Zhang, Y.; Xu, J.; Liu, X.; Liu, K.; Tong, M.; Long, Z. Imidazolium-based ionic porous hybrid polymers with POSS-derived silanols for efficient heterogeneous catalytic CO_2 conversion under mild conditions. *Chem. Eng. J.* **2020**, *381*, 122765. [CrossRef]
41. Guo, Z.; Jiang, Q.; Shi, Y.; Li, J.; Yang, X.; Hou, W.; Zhou, Y.; Wang, J. Tethering dual hydroxyls into mesoporous poly(ionic liquid)s for chemical fixation of CO_2 at ambient conditions: A combined experimental and theoretical study. *ACS Catal.* **2017**, *7*, 6770–6780. [CrossRef]
42. Thommes, M.; Kaneko, K.; Neimark, A.V.; Olivier, J.P.; Rodriguez-Reinoso, F.; Rouquerol, J.; Sing, K.S.W. Physisorption of gases, with special reference to the evaluation of surface area and pore size distribution (IUPAC Technical Report). *Pure Appl. Chem.* **2015**, *87*, 1051–1069. [CrossRef]
43. Xie, Y.; Sun, Q.; Fu, Y.; Song, L.; Liang, J.; Xu, X.; Wang, H.; Li, J.; Tu, S.; Lu, X.; et al. Sponge-like quaternary ammonium-based poly(ionic liquid)s for high CO_2 capture and efficient cycloaddition under mild conditions. *J. Mater. Chem. A* **2017**, *5*, 25594–25600. [CrossRef]

44. Liu, F.; Huang, K.; Wu, Q.; Dai, S. Solvent-free self-assembly to the synthesis of nitrogen-doped ordered mesoporous polymers for highly selective capture andconversion of CO_2. *Adv. Mater.* **2017**, *29*, 1700445. [CrossRef] [PubMed]
45. Ema, T.; Miyazaki, Y.; Shimonishi, J.; Maeda, C.; Hasegawa, J.Y. Bifunctional porphyrin catalysts for the synthesis of cyclic carbonates from epoxides and CO_2: Structural optimization and mechanistic study. *J. Am. Chem. Soc.* **2014**, *136*, 15270–15279. [CrossRef]
46. Luo, R.; Zhou, X.; Chen, S.; Li, Y.; Zhou, L.; Ji, H. Highly efficient synthesis of cyclic carbonates from epoxides catalyzed by salen aluminum complexes with built-in "CO_2 capture" capability under mild conditions. *Green Chem.* **2014**, *16*, 1496–1506. [CrossRef]
47. Zhang, Y.; Yang, D.H.; Qiao, S.; Han, B.H. Synergistic catalysis of ionic liquid-decorated covalent organic frameworks with polyoxometalates for CO_2 cycloaddition reaction under mild conditions. *Langmuir* **2021**, *37*, 10330–10339. [CrossRef]
48. Guo, Z.; Cai, X.; Xie, J.; Wang, X.; Zhou, Y.; Wang, J. Hydroxyl-exchanged nanoporous ionic copolymer toward low-temperature cycloaddition of atmospheric carbon dioxide into carbonates. *ACS Appl. Mater. Interfaces* **2016**, *8*, 12812–12821. [CrossRef]